Semiconductor Science and Technology

PAPER

Donor-acceptor nature of orange photoluminescence in AlN

To cite this article: Ivan A Aleksandrov *et al* 2020 *Semicond. Sci. Technol.* **35** 125006

View the article online for updates and enhancements.

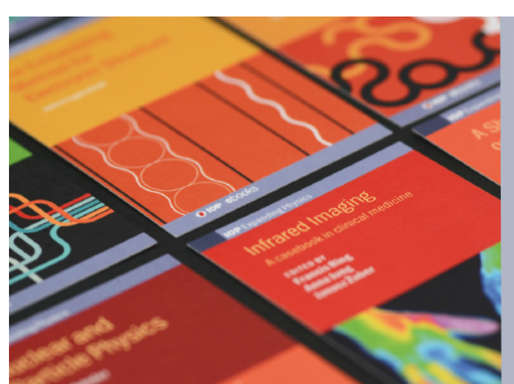

IOP ebooks™

Bringing together innovative digital publishing with leading authors from the global scientific community.

Start exploring the collection–download the first chapter of every title for free.

This content was downloaded from IP address 109.174.115.127 on 28/10/2020 at 10:23

Semicond. Sci. Technol. **35** (2020) 125006 (9pp) https://doi.org/10.1088/1361-6641/abacdd

Donor-acceptor nature of orange photoluminescence in AlN

Ivan A Aleksandrov[1], **Timur V Malin**[1], **Denis S Milakhin**[1], **Boris Ya Ber**[2], **Dmitrii Yu Kazantsev**[2] **and Konstantin S Zhuravlev**[1,3]

[1] Rzhanov Institute of Semiconductor Physics, Novosibirsk, Russia
[2] Ioffe Institute, St. Petersburg, Russia
[3] Novosibirsk State University, Novosibirsk, Russia

E-mail: aleksandrov@isp.nsc.ru

Received 10 May 2020, revised 17 July 2020
Accepted for publication 6 August 2020
Published 13 October 2020

Abstract

Recombination dynamics, photoluminescence and photoluminescence excitation spectra have been investigated for 1.9 eV photoluminescence band in AlN in the temperature range of 5–650 K. The recombination dynamics for the 1.9 eV photoluminescence band has been described by a model of donor-acceptor recombination with taking into account a broadening due to electron coupling with local lattice vibrations of a deep level defect. The experimental results have been compared with density functional theory calculations of luminescence peak energies and line shapes of band to defect and donor-acceptor transitions, and possible origin of the orange photoluminescence band in AlN has been discussed.

Keywords: AlN, photoluminescence, defects

(Some figures may appear in colour only in the online journal)

1. Introduction

III-nitrides and heterostructures based on these materials are technologically important for creating light-emitting diodes and laser diodes of the ultraviolet and visible range [1, 2], high-power high-frequency transistors [3], photodetectors [4, 5], and single-photon sources operating at room temperature [6, 7]. Study of point defects is necessary for control of the material quality, which influences on device performance. Point defects in AlN are manifested in optical experiments, such as luminescence and absorption spectroscopy. Photoluminescence band near 2 eV in AlN was observed in earlier works [8–14]. This band was observed in epitaxial AlN layers as well as in bulk AlN samples with small density of extended defects, which indicates that it is related to point defects. The 2 eV photoluminescence band in AlN has been explained by a transition from a shallow donor to a deep acceptor [11, 12, 14], with ionization energy of the acceptor of 2.4–2.6 eV and Franck-Condon shift of 1.0–1.2 eV. Density functional theory calculations give Franck-Condon shifts for common deep acceptors in AlN in the range 0.34–0.75 eV [15–18]. The observed difference makes it difficult to associate the experimental data on the orange photoluminescence band to the existing calculations of defects in AlN. In order to improve the understanding of the nature of the orange photoluminescence band in AlN, we have investigated this band by stationary and time-resolved photoluminescence spectroscopy and photoluminescence excitation spectroscopy in a wide temperature range of 5–650 K, and have compared the experimental results with density-functional theory calculations of luminescence peak energies and line shapes of band to defect and donor-acceptor transitions taking into account lattice relaxation of both donor and acceptor.

2. Experimental details

AlN samples were grown by molecular-beam epitaxy on (0001) sapphire substrates with ammonia nitrogen source. Undoped AlN sample contains 1.2-μm AlN layer grown at substrate temperature of 940°C ammonia flux of 15 sccm and beam equivalent pressure of Al of 2.0$\cdot$ 10^{-7} Torr. Before

 © 2020 IOP Publishing Ltd Printed in the UK

the start of the growth sapphire substrate was nitrided during 30 min in ammonia flux of 25 sccm at substrate temperature of 840°C. Si-doped AlN sample comprises 1.2-μm Si-doped AlN layer and a 350 nm undoped AlN buffer layer. Doping by silicon during the AlN growth was conducted using a 0.7% silane gas mix with molecular nitrogen at a flux of 3.0 sccm. Nitridation of sapphire substrate was carried out during 9 min in ammonia flux of 25 sccm at substrate temperature of 840°C. The AlN buffer layer was grown at substrate temperature of 940°C at ammonia flux of 10 sccm and beam equivalent pressure of Al of $1.9{\cdot}10^{-7}$ Torr. The Si-doped AlN layer was grown at substrate temperature of 900°C, at ammonia flux of 25 sccm and beam equivalent pressure of Al of $2.3{\cdot}10^{-7}$ Torr. Concentrations of oxygen, carbon and silicon atoms in AlN layers were measured by secondary-ion mass spectrometry (SIMS) in IMS7f (CAMECA) setup with primary Cs^+ ions. Electron beam irradiation was used to neutralize the charge of the samples. The average concentrations of the impurities in the undoped AlN sample are [O] = $1.1{\cdot}10^{21}$ cm^{-3}, [C] = $3.3{\cdot}10^{20}$ cm^{-3}, [Si] = $7.8{\cdot}10^{18}$ cm^{-3}. In the Si-doped AlN layer the average concentrations of the impurities are [O] = $1.0{\cdot}10^{20}$ cm^{-3}, [C] = $8.4{\cdot}10^{19}$ cm^{-3}, [Si] = $1.4{\cdot}10^{20}$ cm^{-3}.

Stationary photoluminescence (PL) spectra of the AlN layers were measured using Acton SP2500i (Princeton Instruments) spectrometer with liquid nitrogen cooled CCD matrix detector. The PL spectra were normalized on spectral sensitivity of the measuring system. The PL was excited by continuous-wave frequency-quadrupled Nd:YAG laser with a photon energy of 4.66 eV for stationary PL spectra and by pulsed frequency-quadrupled Nd:YLF laser with a photon energy of 4.71 eV, pulse duration of 3 ns and pulse repetition frequency of 1 kHz for PL decay kinetics measurements. Diameter of the laser spot was about 0.5 mm in the case of pulsed excitation and about 1 mm in the case of continuous wave excitation. Absorption of the incident light in the AlN layer at the photon energies 4.66–4.71 eV was about 15% for both undoped and Si-doped sample. The time-resolved PL was measured by time-correlated single photon counting system with a cooled FEU-79 photoelectric multiplier working in photon counting mode. For the time-resolved PL a double SDL-1 (LOMO) monochromator was used. Photoluminescence excitation (PLE) spectra were measured using radiation of 450-Watt xenon lamp transmitted through a 350-mm monochromator with a 3600 grooves/mm holographic UV-optimized grating. The radiation power was controlled by a calibrated silicon photodiode. Temperature of the sample was controlled by a helium cryostat for the temperature range 5–325 K, and by a high-temperature thermostat for the temperature range 300–650 K.

3. Results

Figure 1 shows PL and PLE spectra of undoped and silicon-doped AlN samples measured at the temperature of 300 K. A PL band with maximum at 1.93 eV and full width at half maximum (FWHM) of 0.62 eV is observed in the PL spectrum of undoped AlN sample. PLE spectrum of undoped AlN measured at detection energy of 1.93 eV contains a band with maximum at 4.7 eV and FWHM of 1.14 eV. The PL spectrum of silicon-doped AlN contains a band with maximum at 3.09 eV and FWHM of 0.73 eV. A band near 2 eV with interference-modulated shape is also seen in the PL spectrum of the Si-doped AlN sample. PLE spectrum of the Si-doped AlN measured at detection energy of 3.1 eV has a maximum near 6.0 eV which corresponds to interband transition. The 3.1 eV band was studied earlier in [19, 20], so we will focus mainly on the 1.9 eV band in this work.

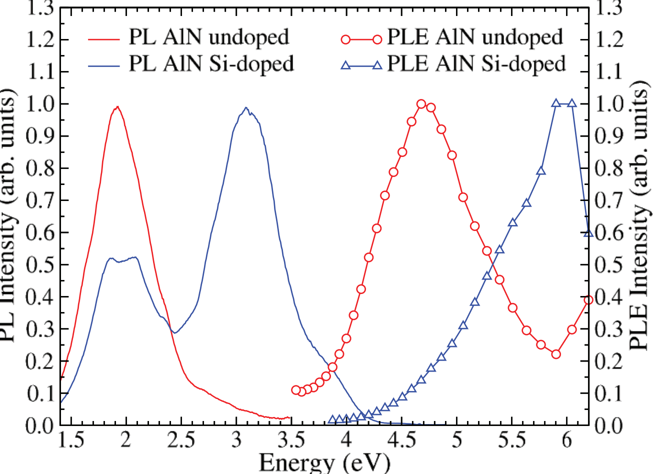

Figure 1. Photoluminescence spectra of undoped and Si-doped AlN samples, measured at the excitation by 4.66 eV laser, and photoluminescence excitation spectra of the same samples, measured at the detection energies of 1.93 eV and 3.1 eV for undoped and Si-doped AlN sample, correspondingly.

Figure 2 shows PL spectra of undoped AlN sample measured at different temperatures at the continuous wave laser excitation with power of 5 mW. PL maximum position remains approximately constant in the temperature range of 5–350 K, and shifts to the higher energies with further increase in the temperature. The temperature dependence of the FWHM of the PL band has been fitted by configuration coordinate model equation [21]:

$$W(T) = W_0\sqrt{\coth\left(\frac{\hbar\omega_{ph}}{2kT}\right)}, \quad (1)$$

where $\hbar\omega_{ph}$ is local phonon energy, and $W_0 = \hbar\omega_{ph}\sqrt{8\ln(2)S}$, S is Huang-Rhys parameter. The fitting gives the values of the parameters $W_0 = 0.56\pm\ 0.01$ eV and $\hbar\omega_{ph} = 51\pm\ 2$ meV. The PL intensity temperature dependence is well described by thermal-activated behavior with two activation energies:

$$I(T) = \frac{I_0}{1 + C_1\exp\left(-\frac{E_{Act1}}{kT}\right) + C_2\exp\left(-\frac{E_{Act2}}{kT}\right)} \quad (2)$$

with parameters $C_1 = 2850\pm\ 10$, $E_{Act1} = 257\pm\ 2$ meV, $C_2 = 0.60\pm\ 0.05$, $E_{Act2} = 10\pm\ 0.5$ meV.

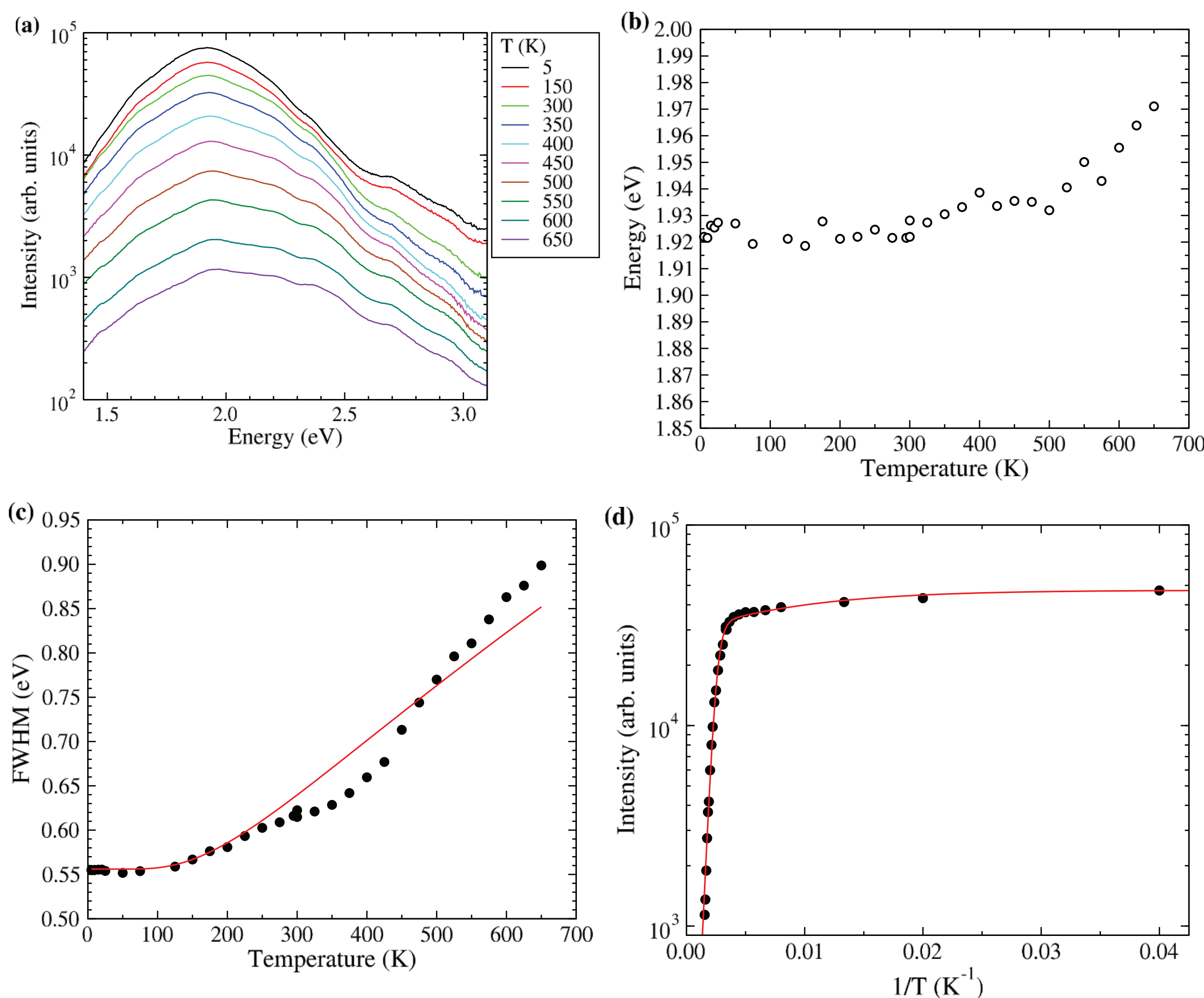

Figure 2. Temperature dependence of the photoluminescence spectrum of undoped AlN (a), and temperature dependences of the PL maximum position (b), full width at half maximum (c), and integrated intensity of the photoluminescence band (d).

Figure 3(a) shows temperature dependence of the PLE spectrum of the undoped AlN sample at the detection energy of 1.93 eV. The PLE spectra were fitted by Gaussian curves, from which the dependences of the width and maximum position of the PLE band have been obtained. At the temperatures higher than 300 K the maximum position of the PLE band shifts to lower energies. This shift is slower than the change in the AlN band gap with the temperature calculated as:

$$E_g(T) = E_g(0) - \frac{2A}{\exp\left(\frac{\Theta}{T}\right) - 1} \qquad (3)$$

with parameters $A = 0.2$ eV, $\Theta = 558$ K [22] (figure 3(b)). The width of the PLE band has been fitted by equation (1), with parameters $W_0 = 1.0$ eV and $\hbar\omega_{ph} = 64$ meV (figure 3(c)).

Figure 4 shows PL decay curves of undoped AlN measured at different photon energies with pulsed laser excitation with average power of 1 mW. The dependence of the PL intensity on time and emission photon energy is well described by the model of donor-acceptor recombination of shallow donor and deep acceptor [23]:

$$I(E,t) = \int_0^\infty I_{E_1}(t) \exp\left(-\frac{(E - E_0 - E_1)^2}{2\Delta^2}\right) dE_1, \qquad (4)$$

where E_0 is a center of Gaussian-shaped vibronic band of a single donor-acceptor pair at the distance between donor and acceptor $r \to \infty$ and Δ is the width parameter of the Gaussian line shape, E_1 is convolution variable, $I_{E1}(t)$ is the time-dependent line shape for the donor-acceptor recombination without taking into account the coupling with local lattice vibrations [24]:

$$I_E(t) = \frac{4\pi n}{E^4}\left(\frac{e^2}{\varepsilon}\right)^3 W_{\max} \exp\left(-\frac{2e^2}{\varepsilon E a_d} - W_{\max} t\right. \\ \left.\exp\left(-\frac{2e^2}{\varepsilon E a_d}\right)\right) \times \exp\left(4\pi n\right. \\ \left.\int_0^\infty \left(\exp\left(-W_R(r)t\right) - 1\right) r^2 dr\right), \qquad (5)$$

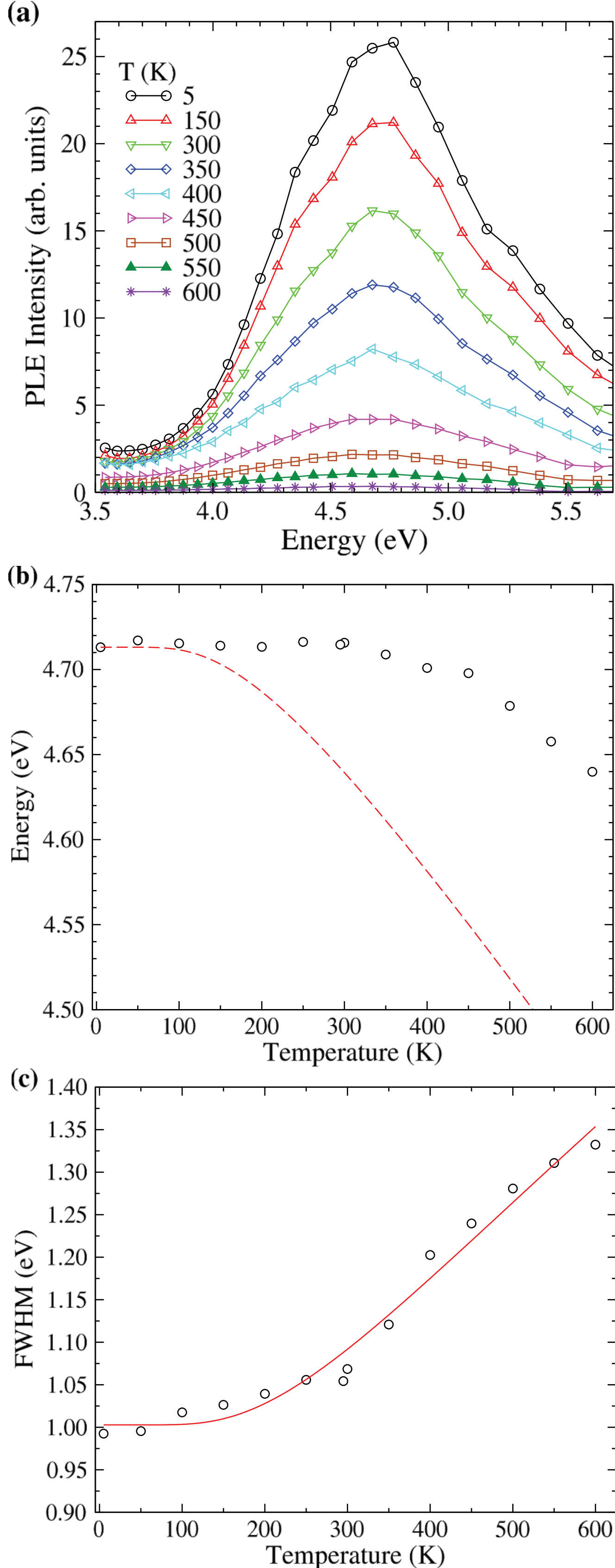

Figure 3. Temperature dependence of the photoluminescence excitation spectrum of undoped AlN measured at detection energy of 1.93 eV (a), and temperature dependences of the maximum position (b) and width (c) of the PLE band. The dashed line shows the change of the AlN band gap with the temperature.

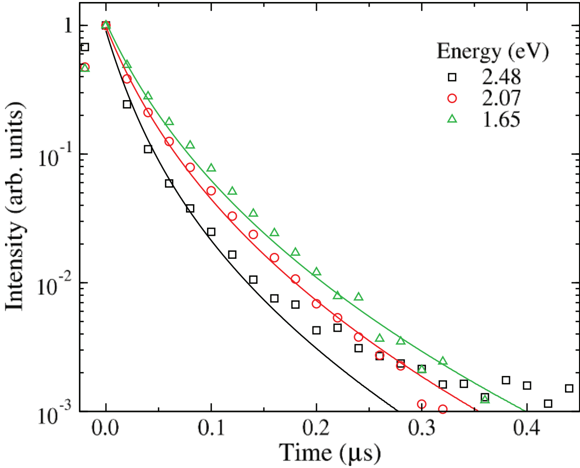

Figure 4. Photoluminescence decay curves of the undoped AlN sample at different spectrum points. Symbols—experiment, solid lines—fitting by equation (4) with fixed value of $a_d = 1.31$ nm and with varying parameters $W_{\max}$ and n, resulting $W_{\max} = 9.6{\cdot}10^7$ s^{-1} and $n = 5.1{\cdot}10^{19}$ cm^{-3}.

$$W_R(r) = W_{\max} \exp\left(-2\frac{r}{a_d}\right), \quad (6)$$

where a_d is donor Bohr radius, r is the distance between donor and acceptor, $W_R(r)$ is the probability of the radiative transition per unit time, ε is dielectric constant, n is concentration of the majority constituent (donors or acceptors). Bohr radius of the shallow donor in the effective mass approximation is $\varepsilon\hbar^2/(m^* e^2)$. With the values of the electron effective mass in AlN $m^* = 0.33m_0$ and dielectric constant $\varepsilon = 8.17$, the donor Bohr radius is $a_d = 1.31$ nm. An estimation of the a_d for the ionization energy assumed to be equal to the activation energy of the PL quenching $E_d = 0.257$ eV is $a_d = 0.67$ nm. The parameters E_0 and Δ were determined by approximation of the stationary PL spectra by the time-integrated equation (4). Fitting of the decay curves in the different spectrum points by the dependence 4 with fixed value of $a_d = 1.31$ nm (figure 4) gives the values of $W_{\max} = 9.6{\cdot}10^7$ s^{-1} and $n = 5.1{\cdot}10^{19}$ cm^{-3}. Fitting of the same curves with fixed value of $a_d = 0.67$ nm gives $W_{\max} = 9.6{\cdot}10^7$ s^{-1} and n = $3.7{\cdot}10^{20}$ cm^{-3}.

In order to verify the model and find a range of possible defect parameters we have compared the experimentally obtained value of $W_{\max}$ with a theoretical estimation. Probability of the donor-acceptor transition per unit time $W_R(r)$ for spin-conserving dipole-allowed transition can be estimated as [25]:

$$W_R(r) \approx \left[\left(\frac{\mathcal{E}_{eff}}{\mathcal{E}_0}\right)^2 n_r\right] \frac{2\alpha\hbar^2\omega^3 E_p}{3m_0c^2E_g^2} I_{DA}^2(r). \quad (7)$$

The overlap integral $I_{DA}(r)$ at $r > a_d > a_a$ can be expressed as [25]:

$$I_{DA}(r) \approx \frac{64(a_a/a_d)^3}{[1-(a_a/a_d)^2]^4} \exp\left(-\frac{2r}{a_d}\right), \quad (8)$$

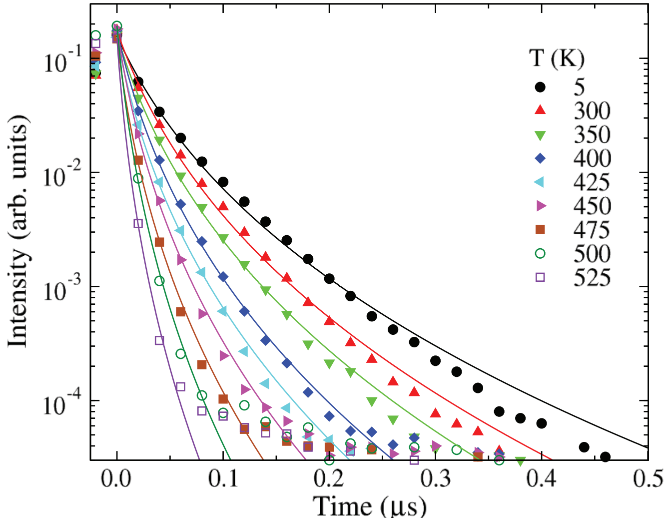

Figure 5. Photoluminescence decay curves for undoped AlN sample at different temperatures. Detection wavelength is 600 nm ($\hbar\omega = 2.07$ eV). Symbols—experiment, solid lines—fitting by equation (4) with varying parameter $W_{\max}$ and fixed values of $a_d = 1.31$ nm and $n = 5.1{\cdot}10^{19}$ cm^{-3}.

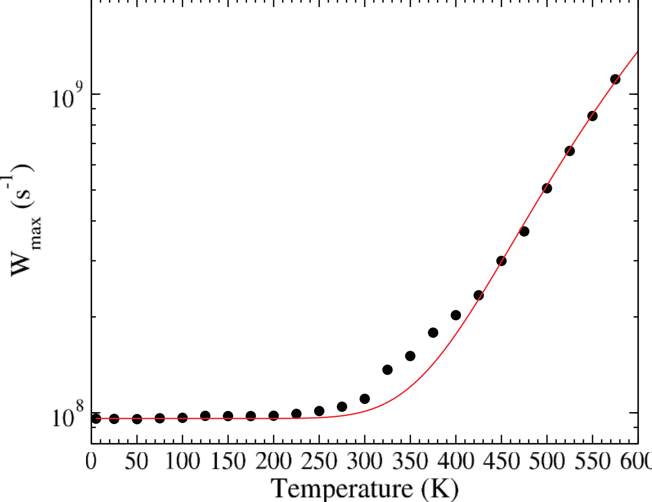

Figure 6. Temperature dependence of the parameter $W_{\max}$ obtained by fitting of the decay curves by the equation (4).

where r is distance between donor and acceptor, a_d and a_a are Bohr radii for donor and acceptor which can be estimated as $a_d = \hbar/\sqrt{2m_e^* E_d}$, $a_a = \hbar/\sqrt{2m_h^* E_a}$. Taking the values of the effective masses of the electron $m_e = 0.33m_0$ [26] and of the light hole $m_h = 0.69m_0$ [26], averaged dielectric constant $\varepsilon = 8.17$ [27], and Kane energy $E_p = 17.8$ eV [26] we obtain for effective mass shallow donor ($E_d = 0.067$ eV) that varying of the acceptor ionization energy E_a from 1.5 eV to 3.5 eV lead to $W_{\max}$ values from $2.6{\cdot}10^7$ s^{-1} to $7.0{\cdot}10^6$ s^{-1}. If we assume $E_d = 0.257$ eV, then varying of the E_a from 1.5 eV to 3.5 eV lead to $W_{\max}$ values from $2.5{\cdot}10^8$ s^{-1} to $5.8{\cdot}10^7$ s^{-1}, which agrees in the order of magnitude with the experimental value of $W_{\max} = 9.6{\cdot}10^7$ s^{-1}. The PL decay time decreases with increase in the temperature (figure 5). It has been empirically found that the decay curves at the different temperatures can be described by equation (4) with the

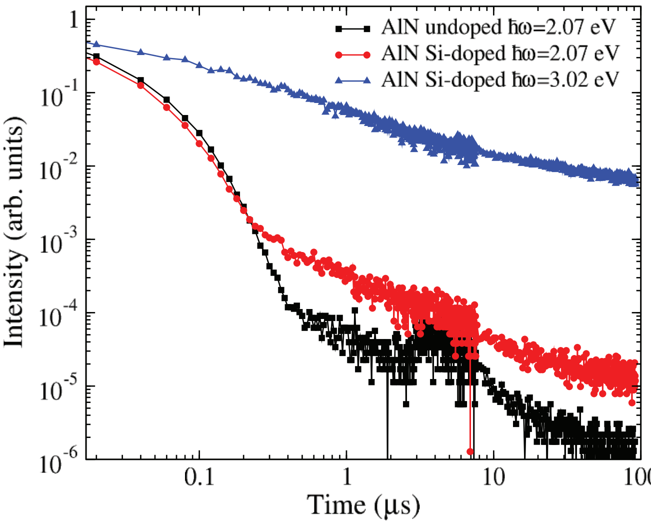

Figure 7. Photoluminescence decay curves of undoped AlN and Si-doped AlN in different spectrum points at the temperature of 300 K.

parameter $W_{\max}$ depending on the temperature as $W_{\max}(T) = W_0 + W_1 \exp(-E_{Act}/kT)$ with activation energy $E_{Act} = 285 \pm 7$ meV (figure 6).

The 3.1 eV PL band in the Si-doped AlN shows much longer decay times and weaker temperature dependence in comparison to the 1.9 eV PL band. The PL intensity of the 3.1 eV band decreases by about 50% with increase in the temperature from 300 K to 650 K with activation energy of 111 meV. Figure 7 shows PL decay curves of the undoped and Si-doped AlN samples. It is seen that the 3.1 eV band decays much slower than the 1.9 eV band. For the 1.9 eV PL band the decay curves of the undoped and Si-doped AlN are very close at the times shorter than 0.3 μs, at the longer times in the Si-doped AlN sample a slower part of the decay curve is observed, which originates from the contribution of the 3.1 eV band.

4. Discussion

In order to improve understanding of the nature of the 1.9 eV photoluminescence band we have conducted density functional theory calculations of the luminescence peak positions and the luminescence line shapes for different defects in AlN [28]. In accordance with previous calculations [15–18], transitions from conduction band to most common acceptors in AlN, such as C_N, V_{Al}, V_{Al}-nO_N, V_{Al}-nSi_{Al} give the PL maximum energy higher than the observed 1.9 eV PL band. Luminescence line shape for donor-acceptor transition, assuming independent local lattice vibrations for donor and acceptor, can be calculated as:

$$G(\hbar\omega) \propto \omega^3 \sum_{j,m,k,l} \mathrm{w}_j(T)\mathrm{w}_k(T)\,|\langle\chi_{ej}|\chi_{gm}\rangle|^2\,|\langle\chi_{el}|\chi_{gk}\rangle|^2 \times G_{DA}\left(\hbar\omega - j\hbar\omega_{ea} + m\hbar\omega_{ga} - k\hbar\omega_{ed} + l\hbar\omega_{gd}\right), \quad (9)$$

where indices j and m numbers initial and final vibrational states of the acceptor with local phonon energies $\hbar\omega_{ea}$ and $\hbar\omega_{ga}$, indices k and l numbers initial and final vibrational states of the donor with local phonon energies $\hbar\omega_{ed}$ and $\hbar\omega_{gd}$, correspondingly. $\mathrm{w}_j(T)$ and $\mathrm{w}_k(T)$ are thermal occupancies of the vibration levels of the acceptor and donor in the initial state, χ_{ej}, χ_{gm}, χ_{el} and χ_{gk} are harmonic oscillator vibrational wave functions for donor and acceptor, and $G_{DA}(\hbar\omega)$ is usual line shape of the donor-acceptor transition without taking into account local lattice vibrations of donor and acceptor [24, 28]. Configuration coordinate model parameters, which determine the vibrational wave functions, were calculated on the basis of the model, proposed by Alkauskas *et al* [29], using density functional theory with hybrid functional HSE [30, 31] with fraction of the Hartree–Fock exchange $a = 0.33$ adjusted to obtain the calculated AlN band gap close to the experimental value.

For donor-acceptor transition from a shallow donor without significant lattice relaxation between the initial and final states to the aluminium vacancy $V_{Al}(2-/3-)$ we have calculated that for the donor ionization energy varying from 50 meV to 300 meV the luminescence peak position varies from 2.93 eV to 2.83 eV, which is about 1 eV higher than the experimental peak position of 1.93 eV. For the defects C_N, V_{Al}-nO_N, C_NO_N, C_NSi_{Al}, V_{Al}-nSi_{Al} the calculated luminescence peak photon energies for donor-acceptor transition from a shallow donor with $E_d = 50$–300 meV are even higher in energy. The calculated low-temperature line widths for band to defect transitions are in the range 0.38–0.53 eV. The widths are increased by about 0.03–0.4 eV for donor-acceptor transitions from a shallow donor with ionization energy of 50–300 meV without taking into account the donor lattice relaxation.

To take into account the donor lattice relaxation we have calculated configuration diagrams of the O_N and Si_{Al} donors in AlN for the charge states 0 and +1. In the charge state +1 of the O_N defect the oxygen atom is located near the N lattice site of the bulk AlN. In the zero charge state the minimum-energy configuration of the O_N defect corresponds to shifted position of the oxygen atom out of the *c* axis. We think that the unshifted position of the oxygen atom in the zero charge state corresponds to shallow donor state with a small Franck-Condon shift, and the minimum-energy configuration corresponds to a deep polaronic state with relatively large Franck-Condon shift. The calculated ionization energy for the minimum-energy configuration of the neutral O_N defect is 0.45 eV and the Franck-Condon shift for transition to +1 charge state is 1.48 eV. Calculated luminescence peak energies for transitions from the minimum-energy configuration of the neutral O_N defect to the C_N, $(V_{Al}3O_N)_c$ and $(V_{Al}3O_N)_a$ defects are 2.19 eV, 2.06 eV and 2.11 eV, correspondingly. Calculated low-temperature line widths for these transitions are in the range of 0.72–0.83 eV, which are higher than the experimental line width 0.56 eV. We think that this difference is caused by assuming the independent lattice relaxations in the equation (9), which leads to overestimation of the line width. Thus, we can suppose that the low emission peak photon energy of the 1.9 eV band can be explained by taking into account the possibility

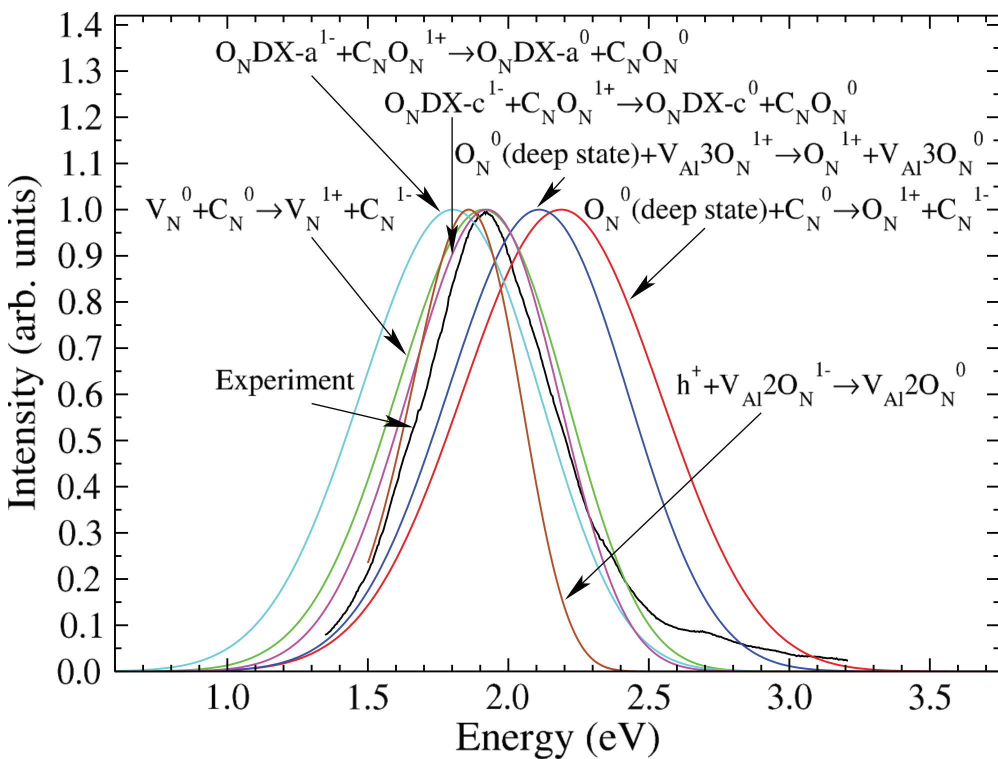

Figure 8. Comparison of the experimental lineshape at T = 10 K for undoped AlN with calculated luminescence lineshapes for different defect-related transitions.

of oxygen donor relaxation into the deep polaronic states with relatively large Franck-Condon shift in the neutral charge state.

Let us consider other possible hypotheses about the nature of the orange photoluminescence band in AlN. According to our calculations, for nitrogen vacancy energy level (0/1+) is located at 1.42 eV below the conduction band edge, and Franck-Condon shift for transition from the neutral charge state to +1 charge state is 0.71 eV. Calculated luminescence peak energy for donor-acceptor transition from $V_N(0/1+)$ to $C_N(0/1-)$ is 1.91 eV, which is in good agreement with the experiment. The calculated line width for this transition is 0.68 eV. The calculated line width for intracentre transition in C_NV_N defect complex is 0.59 eV, which is closer to the experiment. Using the ionization energy $E_d = 1.42$ eV of the $V_N(0/1+)$ donor in the fitting of the PL kinetics, we obtain $n = 3.7\cdot10^{21}$ cm^{-3} and $W_{max} = 1.28\cdot10^8$ s. The high value of the concentration could be explained by supposition that the relative positions of the donors and acceptors are correlated, which leads to shorter average distance between donor and acceptor. However, we expect that at the high concentrations of oxygen and silicon donors the nitrogen vacancies will not be a main donor defect and will have a low concentration.

In the -1 charge state the donors O_N and Si_{Al} form DX-centres with large shifts of the oxygen and silicon atom positions relative to the corresponding lattice site. The calculated luminescence peak energies for transitions from the O_NDX-a and O_NDX-c centres to the C_N defect are 1.54 eV and 1.60 eV. The calculated luminescence peak energies for transitions from the O_NDX-a and O_NDX-c centres to the C_NO_N complex are 1.80 eV and 1.92 eV (figure 8). Thus, the transition from the oxygen DX centres to the C_NO_N complex can be another possible explanation of the orange photoluminescence band in AlN. Considering the transition between donors and defect complexes as acceptors we keep in mind that this is only the simplified way to consider correlation of the defect positions. In general case, different distributions of the atoms in the different lattice sites should be considered.

Another hypothesis is transition of a hole from the valence band to complexes of Al vacancy with oxygen [8]. According to our calculations, the luminescence peak energies for the transition from the valence band to defect is 2.33 eV for $(V_{Al}O_N)_c$, 2.26 eV for $(V_{Al}O_N)_a$, 1.87 eV for $(V_{Al}2O_N)_c$, and 1.86 eV for $(V_{Al}2O_N)_a$, which are comparable to the experimentally observed. However, excitation mechanism for this transition is unclear. It is expected that the Fermi level is in upper half of the band gap in our samples, so the (2−/1−) level for $V_{Al}O_N$ and (1−/0) level for $V_{Al}2O_N$ will be filled and another defect with empty level is needed for creation of a hole in the valence band with below-bandgap excitation. Calculated maximum positions and widths of luminescence bands for all considered transitions at T = 10 K are summarized in the table 1.

We have observed earlier that the intensity of the orange photoluminescence band increases with increase of the III/V flux ratio [11]. Although the intensity is affected by other factors, this general tendency is conserved for a large number of samples. This fact indicates in favor of the defects

Table 1. Calculated maximum positions and widths of luminescence bands for selected donor-acceptor and band to defect transitions in AlN at T = 10 K.

Transition	$\hbar\omega_{PL}$ (eV)	W_0 (eV)
$SD(50-300meV)(0)+V_{Al}(2-)\rightarrow SD(50-300meV)(1+)+V_{Al}(3-)$	2.93–2.83	0.53–0.96
$O_N(0)(deep\,state)+C_N(0)\rightarrow O_N(1+)+C_N(1-)$	2.19	0.83
$O_N(0)(deep\,state)+(V_{Al}3O_N)_a(1+)\rightarrow O_N(1+)+(V_{Al}3O_N)_a(0)$	2.11	0.75
$O_N(0)(deep\,state)+(V_{Al}3O_N)_c(1+)\rightarrow O_N(1+)+(V_{Al}3O_N)_c(0)$	2.06	0.72
$V_N(0)+C_N(0)\rightarrow V_N(1+)+C_N(1-)$	1.91	0.71
$O_NDX_a(1-)+C_N(0)\rightarrow O_NDX_a(0)+C_N(1-)$	1.54	0.66
$O_NDX_c(1-)+C_N(0)\rightarrow O_NDX_c(0)+C_N(1-)$	1.60	0.55
$O_NDX_a(1-)+C_NO_N(1+)\rightarrow O_NDX_a(0)+C_NO_N(0)$	1.80	0.75
$O_NDX_c(1-)+C_NO_N(1+)\rightarrow O_NDX_c(0)+C_NO_N(0)$	1.92	0.62
$h^++(V_{Al}2O_N)_a(1-)\rightarrow(V_{Al}2O_N)_a(0)$	1.86	0.46
$h^++(V_{Al}2O_N)_c(1-)\rightarrow(V_{Al}2O_N)_c(0)$	1.87	0.38
$h^++(V_{Al}O_N)_a(2-)\rightarrow(V_{Al}O_N)_a(1-)$	2.26	0.49
$h^++(V_{Al}O_N)_c(2-)\rightarrow(V_{Al}O_N)_c(1-)$	2.33	0.37
Experiment	1.93	0.56

responsible for the orange band formed in N-lattice site, such as C_N, O_N, V_N, for which the formation energy decreases with the change of the growth conditions from N-rich to Al-rich. Theoretically, concentration of Al vacancies is expected to decrease when the growth conditions are changed from N-rich to Al-rich, however in reference [32] a u-shaped dependence of the Al vacancies concentration on the III/V flux ratio was observed. Taking into account high concentration of oxygen in our samples, we suppose that the donor, responsible for the orange PL band, presumably is O_N. Concentration of donors, obtained from the PL kinetics fit is lower than the oxygen concentration obtained by SIMS. This can be explained by that a part of the oxygen atoms forms complexes with acceptors, such as V_{Al}-nO_N, C_NO_N. The close decay curves for the orange PL band in the undoped AlN sample and the Si-doped AlN sample with lower oxygen concentration can be explained by that the orange PL band in the Si-doped sample originates from the undoped buffer layer.

The maximum position of the photoluminescence excitation band of 4.7 eV is close to the known ultraviolet absorption band in AlN [16], which is related to carbon and was assigned to C_N defect [16], three-carbon [33], and two-carbon [34] complexes. The concentration of the C_N defect is expected to increase with increase in the III/V flux ratio, which agrees with the experimentally observed increase in the luminescence intensity with increase in the III/V flux ratio [11]. The position of the PL excitation band of the 1.9 eV PL band can thus be explained by absorption from the C_N defect to conduction band.

5. Conclusions

In conclusion, photoluminescence, photoluminescence excitation spectra and photoluminescence kinetics have been investigated for the orange photoluminescence band at 1.9 eV in AlN in the wide temperature range of 5–650 K. The recombination dynamics has been described by donor-acceptor recombination model with taking into account local lattice vibrations. In photoluminescence spectrum of silicon-doped AlN another photoluminescence band at 3.1 eV with much slower photoluminescence kinetics is observed. The experimental results have been compared with density-functional theory calculations of the luminescence peak energies for band to defect and donor-acceptor transitions. Calculated luminescence peak energies of the following transitions are relatively close to the experiment: donor-acceptor transition from a shallow donor to $V_{Al}(2-/3-)$, donor-acceptor transition from polaronic state of the O_N neutral donor to C_N and $V_{Al}3O_N$ defects, donor-acceptor transition from the $V_N(0/1+)$ donor to the $C_N(0/1-)$ acceptor, and transition from negatively charged O_N DX-centres to the C_NO_N complex. Large Franck-Condon shift of the orange PL band observed in the experiment can be explained by taking into account lattice relaxation of both donor and acceptor. In our opinion, the most probable explanation of the orange PL band is the recombination from O_N donor to C_N acceptor with correlated relative positions of these defects.

Acknowledgment

This work is supported by the Russian Science Foundation under grant 18-72-00136. The Siberian Branch of the Russian Academy of Sciences (SB RAS) Siberian Supercomputer Centre and Novosibirsk State University are gratefully acknowledged for providing computational resources.

ORCID iDs

Ivan A Aleksandrov https://orcid.org/0000-0001-5481-0971
Timur V Malin https://orcid.org/0000-0001-6015-0631
Denis S Milakhin https://orcid.org/0000-0002-9042-8929
Konstantin S Zhuravlev https://orcid.org/0000-0002-3171-5098

References

[1] Verma J, Kandaswamy P K, Protasenko V, Verma A, Grace Xing H and Jena D 2013 *Appl. Phys. Lett.* **102** 041103
[2] Tanaka S, Lee J S, Ramvall P and Okagawa H 2003 *Japan. J. Appl. Phys.* **42** L885–L887
[3] Mishra U K, Parikh P and Yi-Feng W 2002 *Proc. IEEE* **90** 1022–31
[4] Li J, Fan Z Y, Dahal R, Nakarmi M L, Lin J Y and Jiang H X 2006 *Appl. Phys. Lett.* **89** 213510
[5] Vardi A, Akopian N, Bahir G, Doyennette L, Tchernycheva M, Nevou L, Julien F H, Guillot F and Monroy E 2006 *Appl. Phys. Lett.* **88** 143101
[6] Holmes M J, Choi K, Kako S, Arita M and Arakawa Y 2014 *Nano Lett.* **14** 982–6
[7] Kako S, Santori C, Hoshino K, Götzinger S, Yamamoto Y and Arakawa Y 2006 *Nat. Mater.* **5** 887–92
[8] Sedhain A, Lin J Y and Jiang H X 2012 *Appl. Phys. Lett.* **100** 221107
[9] Schulz T, Albrecht M, Irmscher K, Hartmann C, Wollweber J and Fornari R 2011 *Phys. Status Solidi* b **248** 1513–18
[10] Weinstein I, Vokhmintsev A and Spiridonov D 2012 *Diam. Relat. Mater.* **25** 59–62
[11] Aleksandrov I A, Mansurov V G, Plyusnin V F and Zhuravlev K S 2015 *Physica Status Solidi* C **12** 353–6
[12] Lamprecht M, Grund C, Bauer S, Collazo R, Sitar Z and Thonke K 2017 *Physica Status Solidi (b)* **254** 1600338
[13] Lamprecht M, Jmerik V N, Collazo R, Sitar Z, Ivanov S V and Thonke K 2017 *Phys. Status Solidi* b **254** 1600714
[14] Thonke K, Lamprecht M, Collazo R and Sitar Z 2017 *Phys. Status Solidi* a **214** 1600749
[15] Yan Q, Janotti A, Scheffler M and Van de Walle C G 2014 *Appl. Phys. Lett.* **105** 111104
[16] Collazo R *et al* 2012 *Appl. Phys. Lett.* **100** 191914
[17] Lyons J L, Janotti A and Van de Walle C G 2014 *Phys. Rev.* B **89** 035204
[18] Harris J S *et al* 2018 *Appl. Phys. Lett.* **112** 152101
[19] Osinnykh I V, Malin T V, Plyusnin V F, Suranov A S, Gilinsky A M and Zhuravlev K S 2016 *Japan. J. Appl. Phys.* **55** 05FG09
[20] Osinnykh I V, Malin T V, Milakhin D S, Plyusnin V F and Zhuravlev K S 2019 *Japan. J. Appl. Phys.* **58** SCCB27
[21] Klick C C and Schulman J H 1957 Luminescence in solids *Solid State Physics* Seitz F and Turnbull D vol 5 (New York: Academic) pp 97–172
[22] Feneberg M, Leute R A R, Neuschl B, Thonke K and Bickermann M 2010 *Phys. Rev.* B **82** 075208
[23] Goldys E M, Godlewski M, Langer R, Barski A, Bergman P and Monemar B 1999 *Phys. Rev.* B **60** 5464–9
[24] Thomas D G, Hopfield J J and Augustyniak W M 1965 *Phys. Rev.* **140** A202–A220
[25] Barry W A and Watkins G D 1996 *Phys. Rev.* B **54** 7789–98
[26] Rinke P, Winkelnkemper M, Qteish A, Bimberg D, Neugebauer J and Scheffler M 2008 *Phys. Rev.* B **77** 075202
[27] Feneberg M, Romero M F, Röppischer M, Cobet C, Esser N, Neuschl B, Thonke K, Bickermann M and Goldhahn R 2013 *Phys. Rev.* B **87** 235209
[28] Aleksandrov I A and Zhuravlev K S 2020 *J. Phys. Cond. Matter* **32** 435501
[29] Alkauskas A, Lyons J L, Steiauf D and Van de Walle C G 2012 *Phys. Rev. Lett.* **109** 267401
[30] Heyd J, Scuseria G E and Ernzerhof M 2003 *J. Chem. Phys.* **118** 8207–15
[31] Heyd J, Scuseria G E and Ernzerhof M 2006 *J. Chem. Phys.* **124** 219906
[32] Koyama T, Sugawara M, Hoshi T, Uedono A, Kaeding J F, Sharma R, Nakamura S and Chichibu S F 2007 *Appl. Phys. Lett.* **90** 241914
[33] Irmscher K, Hartmann C, Guguschev C, Pietsch M, Wollweber J and Bickermann M 2013 *J. Appl. Phys.* **114** 123505
[34] Gamov I, Hartmann C, Wollweber J, Dittmar A, Straubinger T, Bickermann M, Kogut I, Fritze H and Irmscher K 2019 *J. Appl. Phys.* **126** 215102